An experimental analysis of canopy flows

Journal of Physics: Conference Series **318** (2011) 072018 doi:10.1088/1742-6596/318/7/072018

An experimental analysis of canopy flows

Antonio Segalini, Jens H. M. Fransson & P. Henrik Alfredsson
Linné FLOW Centre, KTH Mechanics, SE-100 44 Stockholm, Sweden
E-mail: segalini@mech.kth.se

Abstract. An analysis of forest canopy flows with a wind tunnel model at high Reynolds number is presented and discussed. Measured mean velocity and Reynolds stress profiles agree with observations made in real canopies with no sensible Reynolds number dependence, adding confidence to the results obtained with the present setup. The analysis of power density spectra of the three velocity components and of the shear stress co-spectra is reported with new coordinate scalings able to improve the collapse of the spectra compared to standard normalizations. This scaling is mostly based on the respective integral time scale and a simple fit is proposed to estimate such a quantity in real canopies. From the analysis of joint probability density functions, three different regions have been localized where a change in the coherent structure behavior is supposed to take place, similarly to what happens in rough wall turbulent boundary layers.

1. Introduction

There is a renewed interest in the description of the atmospheric boundary layer over forest areas due to the strong exploitation of wind energy in Europe but also elsewhere. From the power production point of view, wind turbine parks located on flat land or at sea are more ideal as compared to locations in forest areas, but the number of such exploitable areas is limited. Therefore great efforts are spent to characterize the effect of the presence of a forest canopy in order to assess wind turbine performance (in terms of extracted power and fatigue loads) and, therefore, the quality of a given site.

Measurements in the atmospheric boundary layer over a forest canopy are affected by several issues, such as diurnal variations of both wind velocity, wind direction and stratification (Kaimal & Finnigan, 1994). The non-homogeneity of any forest canopy and the measurement uncertainties add further complications to the evaluation and the quality assessment of the data. While the validity of the predictions of numerical methods is still a matter of debate due to modeling issues, wind tunnel experiments, which ensure a better control of the operating conditions, are a good alternative to field measurements to obtain a physical understanding of the most important processes. However the Reynolds numbers achievable are of the order of one hundred times smaller compared to those of the atmospherical boundary layer, but may still be sufficiently high to give a qualitatively correct description of the flow processes. These considerations justify the considerable number of wind tunnel experiments with simplified canopy models (see Meroney, 1968; Zhu *et al.*, 2006; Pietri *et al.*, 2009, to cite some), with a reasonable agreement of the measured data with the ones acquired over a real canopy (Zhu *et al.*, 2006; Novak *et al.*, 2000).

What seems to be clear from theory and experiments is that the presence of the canopy introduces a nonlinear momentum sink term in the Navier-Stokes equations, with a consequent change in the flow characteristics inside the canopy and in the neighborhood of the canopy top, phenomena completely absent in smooth wall turbulent boundary layers. It has only been recently assessed that the presence of the forest is related to an inflectional point in the mean velocity profile (Raupach *et al.*, 1996) located in the proximity of the canopy top. From the Rayleigh inflectional point criterion it is expected that the canopy flow is unstable to inviscid perturbations and that a Kelvin-Helmholtz instability develops close to the inflectional point. Consequently the roll-up and generation of coherent vortices is localized near the canopy interface, while the dynamics of these structures will be seen across the full height of the boundary layer. The effect of such an instability and the dynamics of the generated structures is still unclear and therefore a wind tunnel experiment has been performed in order to describe the flow from the classical statistical point of view. The statistical results will be discussed in the present work where single-point measurements will be analyzed.

The paper is structured in the following way: first the experimental setup is briefly described in section 2 after which the presentation and discussion of the experimental results will be done in section 3. Section 4 concludes the paper by summarizing the most important results achieved.

2. Experimental setup

The experiments have been performed in the Minimum Turbulence Level wind tunnel (MTL) at the Royal Institute of Technology (KTH) in Stockholm. The facility has a closed-loop configuration with a 7 m long test section and a cross section with 1.2 m width and 0.8 m height.

Figure 1 shows a schematic representation of the model setup in the wind tunnel test section. The atmospheric boundary layer is simulated by means of triangular spires at the beginning of the test section to artificially increase the boundary layer thickness up to 0.5 m (Talamelli *et al.*, 2004). In order to simulate a forest canopy four pin fin plates with a width of 1.2 m and a streamwise length of 0.5 m each have been used. The trees of the canopy have been simulated by 5 mm diameter wooden circular pins that have been mounted in holes in the plates, where the tip of the pins reaches 50 mm above the plate. The pins can be removed or added in order to create canopies with different densities. The height of the canopy is indeed $h_c = 50$ mm while the length of the total forest model is 40 canopy heights. The high pin density (1700 pins/m^2) ensures homogeneity in both streamwise and spanwise direction. The reference frame used in the present paper is schematically shown in figure 1. As a notation, the streamwise velocity will be denoted with u, the wall-normal with v and the spanwise with w. Also, capital letters will indicate statistically averaged quantities, while lower case letters will indicate fluctuations around the mean value.

Hot-wire anemometry has been used during the experimental campaign to determine statistical properties of the flow. The use of crossed-hot-wire sensors has allowed simultaneous measurements of two velocity components. By rotating the wires by 90°, statistics of all the three velocity components have been determined. Time series have been acquired for four different free-stream velocities ($U_\infty \approx 10$, 15, 20 and 25 m/s) at 20 points across the boundary layers with a sampling frequency of 20 kHz and a sampling time of 100 s in order to achieve a good statistical convergence and to acquire enough structures for the ensemble average.

3. Results

Figure 2 reports the mean velocity profile (a) and the most important Reynolds stress profiles (b) for the different free-stream velocities available at the streamwise station $x/h_c = 30$: both quantities, if appropriately scaled with U_∞, show a weak Reynolds number dependence, therefore

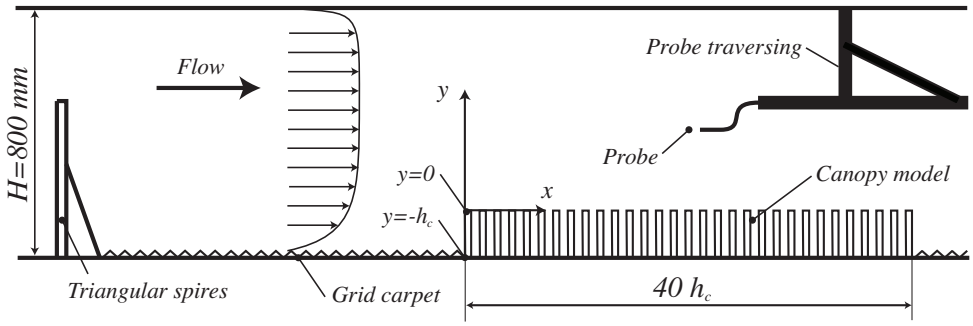

Figure 1. Schematic representation of the wind tunnel canopy model setup.

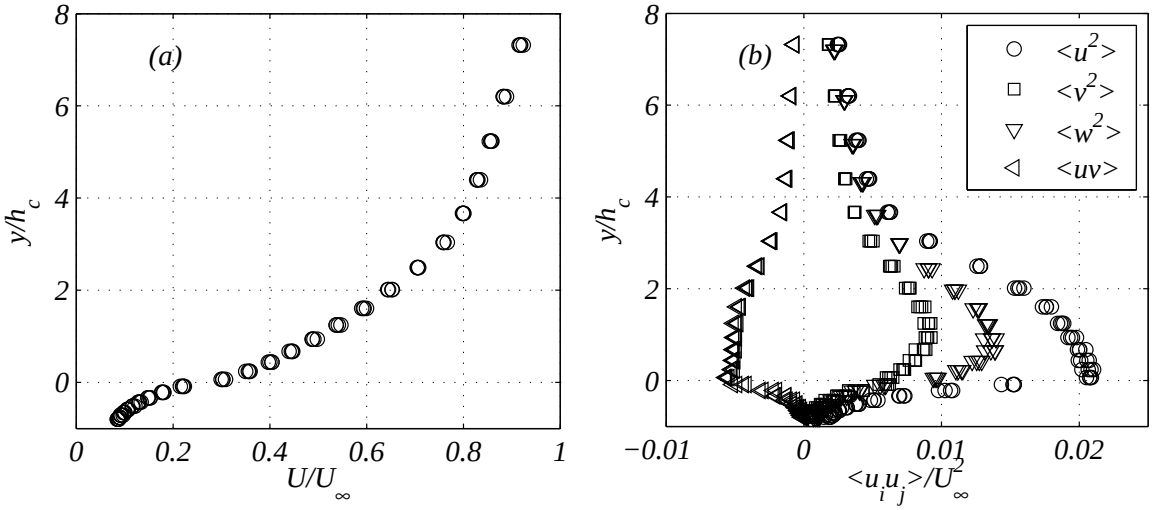

Figure 2. Statistics of the low density canopy flow for $10 < U_\infty < 25$ m/s. (a) Mean velocity profiles (b) variances of the three velocity components and $\langle uv \rangle$ covariance profiles.

the flow can be considered as Reynolds number independent. Inside the canopy (i.e. for $y < 0$), the mean velocity decays exponentially, in agreement with atmospherical measurements inside forests and with some theoretical models (Harman & Finnigan, 2007), while the inflectional point is located at the canopy interface (Raupach *et al.*, 1996). Above the canopy the logarithmic law is recovered, provided that y is shifted by some displacement height. The normal turbulent stresses decay inside the canopy from their maxima achieved close to the canopy top, above which a region of approximately constant shear and normal stress is observed.

Spectral analysis has been performed to the velocity time series, calculating both power spectral density of all the three velocity components (P_u P_v P_w) and the real part of the cross-spectra (S_{uv} usually called co-spectra). All the spectra have been normalized in order to ensure a constant area underneath and a constant value for zero frequency. This can be accomplished by starting from the definition of cross-correlation between the time series $u(t)$ and $v(t)$ (the case where $v = u$ is a special one and follows the same arguments):

$$R_{uv}(\tau) = \langle u(t)\, v(t+\tau) \rangle \ . \tag{1}$$

The application of the Wiener-Kinchine theorem (Bendat & Piersol, 1986) relates the cross-

correlation (1) with the cross-spectra as:

$$S_{uv}(f) = \int_{-\infty}^{+\infty} R_{uv}(\tau)\, e^{-2\pi i f \tau} d\tau \qquad R_{uv}(\tau) = \int_{-\infty}^{+\infty} S_{uv}(f)\, e^{2\pi i f \tau} df\,. \tag{2}$$

From equation (2) the value of the spectra in $f = 0$ is calculated as:

$$S_{uv}(0) = \int_{-\infty}^{+\infty} R_{uv}(\tau)\, d\tau = 2\langle uv\rangle \Lambda_{uv} \qquad \text{with} \qquad \Lambda_{uv} = \frac{1}{2\langle uv\rangle}\int_{-\infty}^{+\infty} R_{uv}(\tau)\, d\tau\,. \tag{3}$$

The introduction of the integral time scale Λ_{uv} is usually made for the auto-correlations, but the argument is here generalized provided that $\langle uv\rangle \neq 0$. A normalized spectra can be now defined as:

$$\Phi_{uv}(f) = \frac{S_{uv}(f)}{\langle uv\rangle \Lambda_{uv}}\,, \tag{4}$$

that, according to equation (3), satisfies $\Phi_{uv}(0) = 2$ and:

$$\frac{1}{\langle uv\rangle}\int_{-\infty}^{+\infty} S_{uv}(f)\, df = \int_{-\infty}^{+\infty} \Phi_{uv}(f\Lambda_{uv})\, d(f\Lambda_{uv}) = 1\,. \tag{5}$$

Equation (5) suggests that the scaled spectra (4) normalizes the spectra at $f = 0$ and the integral of the spectra through the use of the frequency scaled with the integral time scale, Λ_{uv}. The advantage of the proposed normalization is evinced when the spectra depends on a single length and velocity scale, allowing a universal description of the spectra, independently from the wall-normal position, y, or free-stream velocity, U_∞.

Figures 3 and 4 report normalized spectra of the three velocity components and the real part of the cross-spectra, S_{uv}, for all the available free-stream velocities for $0 < y/h_c < 3.6$. The upper limit $y/h_c \approx 3.6$ is the edge of the internal canopy boundary layer above which the external replicated atmospherical boundary layer starts (this can be appreciated for instance in the skewness profiles in figure 6(a) or by looking at the evolution of the statistics along the canopy model, not shown here). Therefore below this threshold the flow is expected to be determined by the canopy boundary condition, while above it is dominated by the way used to generate the thick boundary layer, with a different expected spectral distribution. In the canopy boundary layer (for $0 < y/h_c < 3.6$) the collapse of all the spectra up to the dissipative range (i.e. for $f\Lambda \gg 1$) is evident. In order to facilitate the quantitative comparison of the normal stress spectra, they have been plotted together with a fit of Φ_u in the inertial range. All the normal spectra show the Kolmogorov $-5/3$ decay for all the considered y positions inside the internal canopy boundary layer. The spectra reported in figure 3 are plotted together with the spectral distribution $\Phi = (f\Lambda)^{-5/3}/18$ which is a fit of the streamwise velocity spectrum estimated from the wind tunnel data but the same fit has been recently found in real forest data (Segalini *et al.*, 2011). The cross-spectra, on the other hand, show a faster decay and some zero crossings in the high frequency range, adding further scatter in the logarithmic plot in figure 4(a). This quicker decay is however consistent with the expected frequency decay of the co-spectra in the inertial range (Kaimal & Finnigan, 1994), namely $f^{-7/3}$ (shown in figure 4), even if a decay between $f^{-5/3}$ and $f^{-7/3}$ seems to fit more appropriately the spectra.

It is interesting now to evaluate the integral time scales Λ_x as function of simple parameters. In the previous figures they have been calculated directly from the definition in equation (3), since the sampling time in the wind tunnel experiment was sufficiently high, but real atmospheric measurements have only a limited time window where the flow can be considered as statistically stationary. It is therefore of use to propose a simple correlation from the present experimental

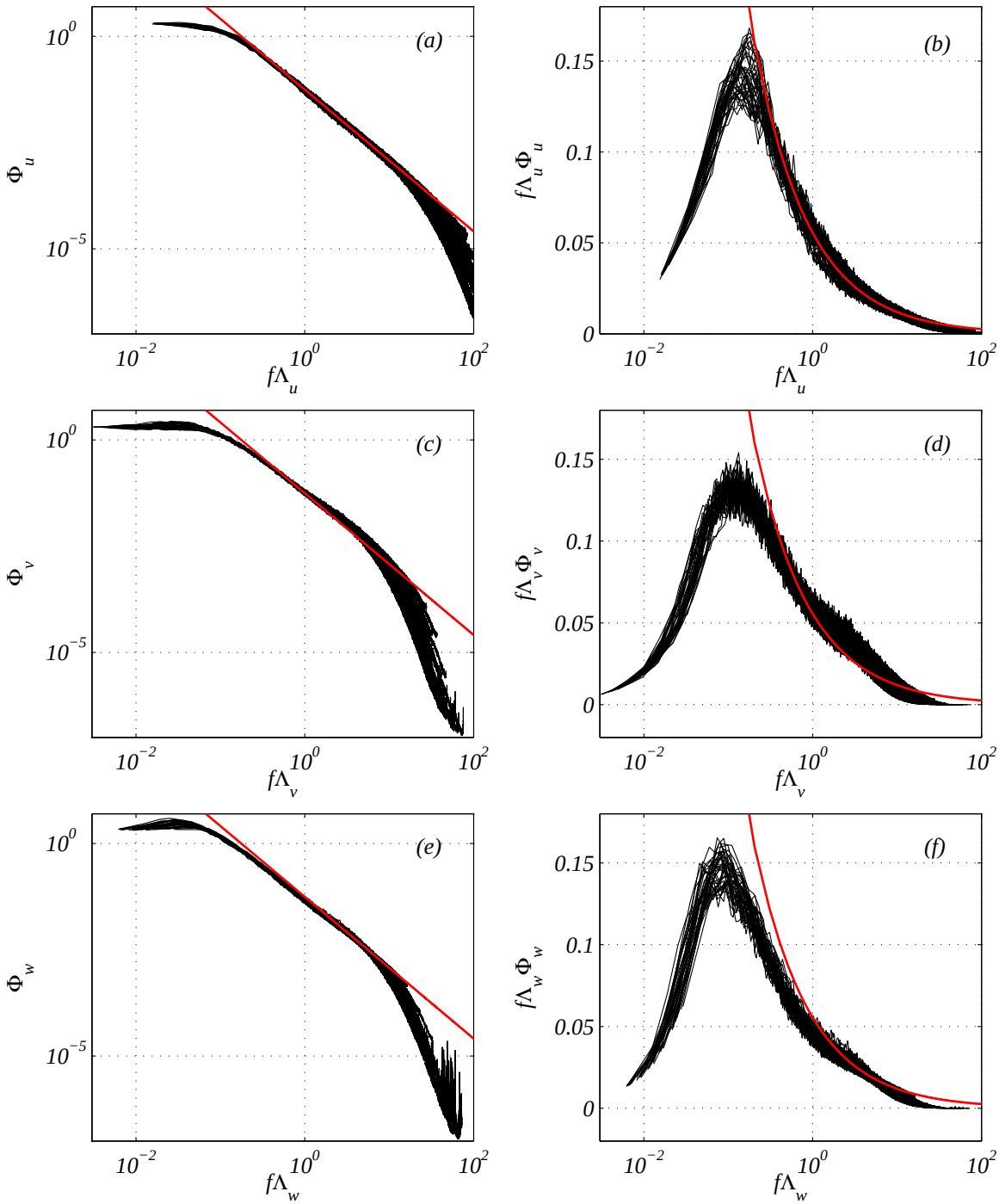

Figure 3. Normalized power density spectra of the $(a-b)$ u, $(c-d)$ v and $(e-f)$ w velocity component for $10 < U_\infty < 25$ m/s and $0 < y/h_c < 3.6$. $(a-c-e)$ Non premultiplied form, $(b-d-f)$ premultiplied form. For comparison purposes the function $\Phi = (f\Lambda)^{-5/3}/18$ is plotted (solid red line).

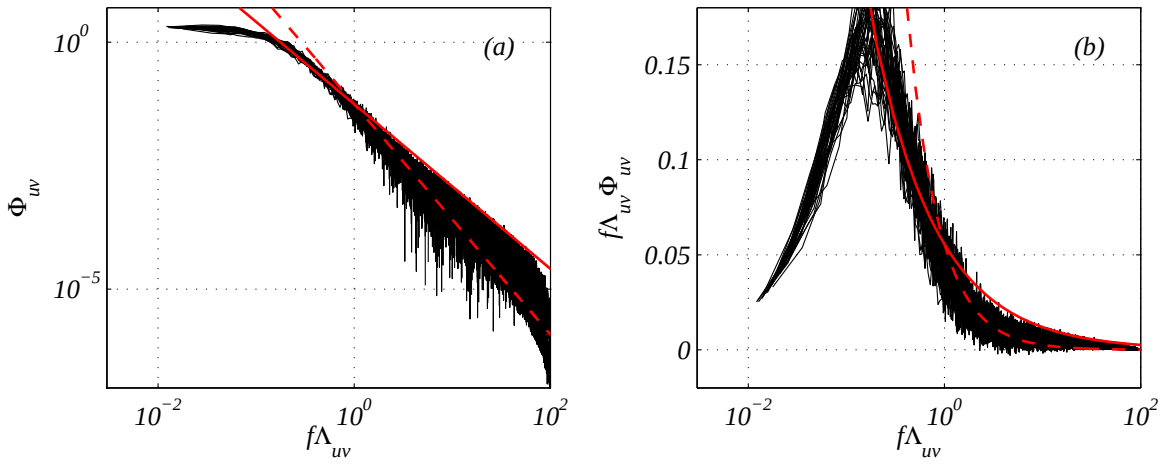

Figure 4. Normalized co-spectra S_{uv} for $10 < U_\infty < 25$ m/s and $0 < y/h_c < 3.6$. (a) Non premultiplied form, (b) premultiplied form.. For comparison purposes the functions $\Phi = (f\Lambda)^{-5/3}/18$ (solid red line) and $\Phi = (f\Lambda)^{-7/3}/18$ (dashed red line) are plotted.

results able to estimate an approximative value of the integral time scales. Dimensional analysis, and some change of variables, suggests a possible relationship of the form:

$$\frac{y}{\Lambda_x U} = A_x + B_x \frac{U}{U_\infty}\,, \tag{6}$$

where, instead of a y-dependent right hand side, a correlation with U/U_∞ has been preferred following the idea of the diagnostic plot approach proposed by Alfredsson *et al.* (2011). Figure 5 reports the proposed relationship for Λ_u, Λ_v and Λ_{uv}. The agreement of the linear fit with the measured data can be judged as good above the canopy. It is worth to mention that Λ_w has not been plotted because the data agree with Λ_v but they are more scattered and therefore have been omitted for clarity. It is also interesting to note that for homogeneous isotropic turbulence $\Lambda_v = \Lambda_w = \Lambda_u/2$ (Pope, 2000), while here it seems that $\Lambda_v \approx \Lambda_u/4$. Another simple scaling that can be used is $\Lambda_u U_h/h_c \approx 1.2$ with $U_h = U\,(y = 0)$. However this scaling seems to work only for the integral time scale of the streamwise velocity component, while the vertical velocity integral scale shows a clear y-dependent trend.

A further statistical description of the flow events can be obtained by quadrant analysis of the velocity time series. It is known that in smooth wall turbulent boundary layers ejections ($u < 0$ and $v > 0$) are the most probable events. On the other hand, in rough wall turbulent boundary layers sweeps ($u > 0$ and $v < 0$) are the most probable events close to the roughness (Krogstad *et al.*, 1992) while away from it ejections become again the most probable events. This property is also observed in canopy flows (Shaw *et al.*, 1995) and in the present model as can be evinced from figure 6 where the skewness of the streamwise and wall-normal velocity is reported in part (a) while parts (b), (c) and (d) show the joint probability density function at $y/h_c \approx 0$, $y/h_c \approx 1$ and $y/h_c \approx 3.6$, respectively. The first location corresponds to the canopy interface where sweeps are expected to be dominant and the joint pdf appears strongly skewed for both axes. At $y/h_c \approx 1$ the skewness of u and v is approximately zero and the joint probability function is centered at the origin and symmetric. In the last station, ejections take place but the joint pfd appears only slightly asymmetric with a maximum in the fourth quadrant, underlining the complex structure of the canopy flow and some analogies with rough wall studies. It is worth to note that in each plot reported in figure 6 statistics with four different

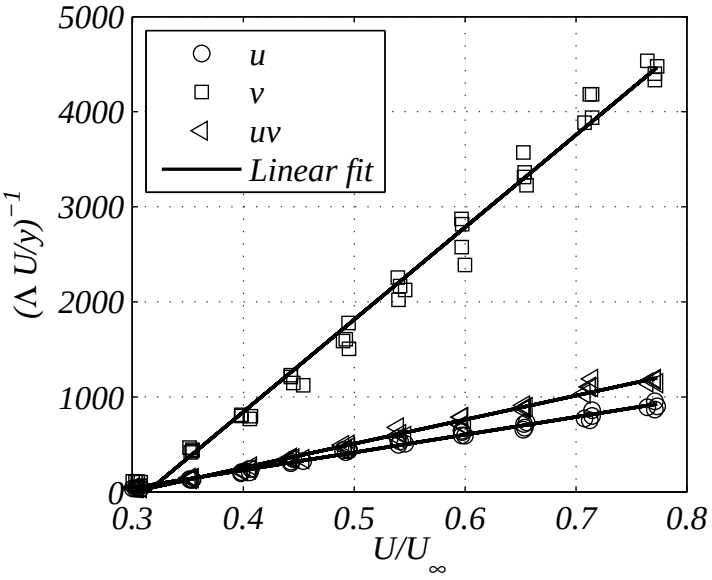

Figure 5. Distribution of $(\Lambda U/y)^{-1}$ as a function of U/U_∞.

free-stream velocities have been plotted confirming that Reynolds number effects are negligible above the canopy layer.

4. Conclusions

An experimental analysis of canopy flows has been performed and discussed. The canopy flow has been artificially reproduced in a wind tunnel in order to achieve a similar description of what is happening in a real forest. Most of the experimental results of the present work are in agreement with the ones observed by other researchers in both field experiments and numerical simulations (Raupach *et al.*, 1996; Finnigan, 2000) underlining the fact that the present simplified canopy model is able to replicate realistically what happens in a real forest.

An analysis of the statistics measured at $x/h_c = 30$ shows no Reynolds number dependence (despite the change of U_∞ of a factor three). The flow can be subdivided in three regions, namely the one below the canopy interface (where a decay of the turbulence with y is observed), the region just above the canopy interface (where a constant stress layer is usually assumed to be present) and the region above the internal canopy boundary layer (where the present flow is affected by the spires used to artificially increase the thickness of the incoming boundary layer).

The new scaling of the velocity spectra with the integral time scale has shown a remarkable collapse of the spectra over the vertical extension of the canopy boundary layer, demonstrating scale separation by two frequency decades. All the power density spectra of the three velocity components agree with the Kolmogorov $f^{-5/3}$ law, with some small discrepancy in the v and w spectra. The co-spectra relative to the covariance uv show a turbulence decay between $f^{-5/3}$ and the theoretically predicted $f^{-7/3}$. A linear relationship between the normalized integral time scale and the mean velocity has been proposed in order to facilitate the estimation of the integral time scales in real canopies where the evaluation of such quantities is complicated by the lack of a sufficient statistical convergence.

The analysis of the skewness profiles and of the joint probability density functions at some key points have highlighted the changes in the structure behavior across the canopy boundary layer. Namely, close to the canopy interface sweeps are likely to occur, with patches of high speed fluid

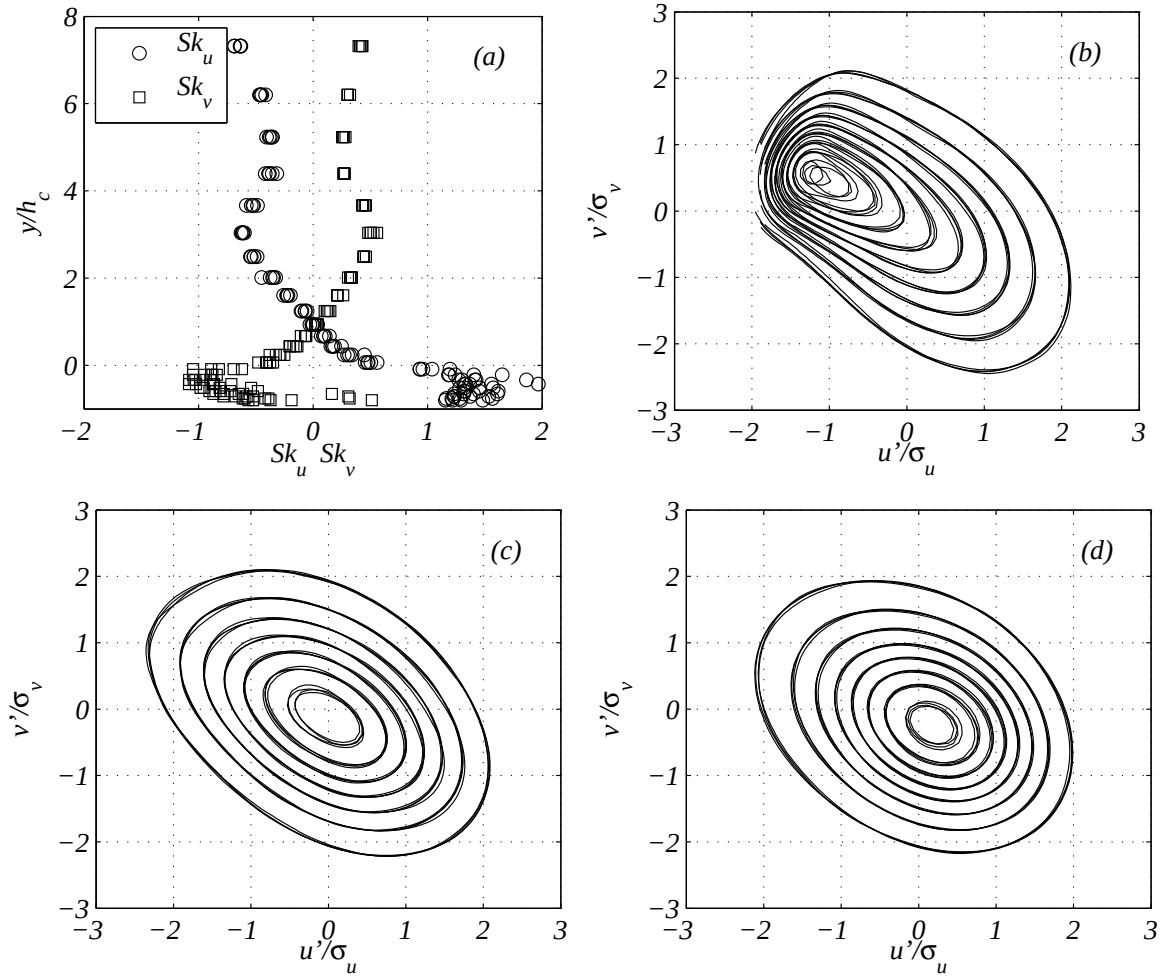

Figure 6. (a) Skewness profile of u and v for $10 < U_\infty < 25$ m/s. Normalized joint pdf uv for $10 < U_\infty < 25$ m/s at (b) $y/h_c \approx 0$, (c) $y/h_c \approx 1$ and (d) $y/h_c \approx 3.6$. The iso-levels starts from 0.02 with steps of 0.02.

going inside the canopy region from above, while far from the canopy classical ejections take place, with patches of low speed fluid going towards the outer region of the boundary layer. This behavior is analogous to rough wall turbulent boundary layers, where this structure dynamics change has also been observed with quadrant analysis methods.

This work is part of Vindforsk III, a research program sponsored by the Swedish Energy Agency. The authors wish to thank Dr. Ebba Dellwik for the useful comments during the preparation of the present manuscript.

References

Alfredsson, P. H., Segalini, A. & Örlü, R. 2011 A new scaling for the streamwise turbulence intensity in wall-bounded turbulent flows and what it tells us about the outer peak. *Phys. Fluids* **23**, 041702.

Bendat, J. S. & Piersol, A. G. 1986 *Random data*, 2nd edn. USA: John Wiley & Sons.

Finnigan, J. J. 2000 Turbulence in plant canopies. *Annu. Rev. Fluid Mech.* **32**, 519–571.

Harman, I. N. & Finnigan, J. J. 2007 A simple unified theory for flow in the canopy and roughness sublayer. *Bound. Lay. Meteorol.* **123**, 339–363.

Kaimal, J. C. & Finnigan, J. J. 1994 *Atmospheric boundary layer flows. Their structure and measurement*. Oxford University press.

Krogstad, P. Å., Antonia, R. A. & Browne, L. W. B. 1992 Comparison between rough- and smooth-wall turbulent boundary layers. *J. Fluid Mech.* **245**, 599–671.

Meroney, R. N. 1968 Characteristics of wind and turbulence in and above model forests. *J. Applied Meteorology* **7**, 780–788.

Novak, M. D., Warland, J. S., Orchansky, A. L., Ketler, R. & Green, S. 2000 Wind tunnel and field measurements of turbulent flow in forests. part 1: Uniformly thinned stands. *Bound. Lay. Meteorol.* **45**, 457–495.

Pietri, L., Petroff, A., Amielh, M. & Anselmet, F. 2009 Turbulence characteristics within sparse and dense canopies. *Environ. Fluid Mech.* **9**, 297–320.

Pope, S. B. 2000 *Turbulent flows*. Cambridge university press, UK.

Raupach, M. R., Finnigan, J. J. & Brunet, Y. 1996 Coherent eddies and turbulence in vegetation canopies: the mixing-layer analogy. *Bound. Lay. Meteorol.* **78**, 351–382.

Segalini, A., Arnqvist, J. & Dellwik, E. 2011 Universality issues in forest canopies. *Bound. Lay. Meteorol. (manuscript in preparation)* .

Shaw, R. H., Brunet, Y., Finnigan, J. J. & Raupach, M. R. 1995 A wind tunnel study of air flow in waving wheat: two-point velocity statistics. *Bound.-Lay. Meteorol.* **76**, 349–376.

Talamelli, A., Riparbelli, L. & Westin, K. J. A. 2004 An active grid for the simulation of atmospheric boundary layers in a wind tunnel. *Wind Struct.* **7**, 131–144.

Zhu, W., van Hout, R., Luznik, L., Kang, H. S., Katz, J. & Meneveau, C. 2006 A comparison of piv measurements of canopy turbulence performed in the field and in a wind tunnel model. *Exp. Fluids* **41**, 309–318.